DOI: 10.13009/EUCASS2017-291



# Buffet suppression by submicrosecond spark discharge

*Aleksandr Firsov*, Yuriy Isaenkov*, Sergey Leonov*[#], Ivan Moralev*, Vitaly Soudakov[§]*
**Joint Institute for High Temperatures RAS, Moscow, 125412, Russia*
*[#]University of Notre Dame, Notre Dame, Indiana, 46556, USA*
*[§]Central Aerohydrodynamic Institute (TsAGI), Zhukovsky, Moscow Region, 140180, Russia*

## Abstract

This work considers the results of experimental and numerical study of implementation of plasma-based flow actuators for control of transonic buffet phenomenon. Actuators based on submicrosecond multispark array were considered. It was demonstrated that the spark plasma actuator could significantly reduce amplitude of shock oscillations over the wing model.

## 1. Introduction

This paper is focused on experimental and computational study of effect of submicrosecond multispark plasma array actuators on the buffet phenomenon in transonic flow. At cruise speed of atmospheric flight at Mach number M=0.72-0.85 and/or high angle of attack an unsteady pattern of the transonic flow can be realized on the upper side of an airfoil. The flow deceleration in the boundary layer can induce a boundary layer separation in a region of strong shock wave/boundary layer (SWBL) interaction and can results in a high-magnitude oscillation of the shock wave that greatly affects the aircraft aerodynamics through the lift and drag unsteadiness. This phenomenon is known as "buffet" and can further lead to structural vibrations, which are called "buffeting".
Previously, different types of flow control technique have been considered in experimental studies and in numerical modeling (CFD) for buffet delay: mechanical vortex generators placed upstream of a major transonic shock position [1, 2]; fluidic vortex generators [3, 4]; shock control bumps located at the shock position [1, 5, 6]; trailing edge deflector - moving part, sited at the trailing edge of the wing [1, 7, 8] etc. Those results demonstrate that described mechanical and fluidic actuators are able to suppress the massive flow separation, which occurs without flow actuation, and to prevent the shock-induced oscillation. On the other hand, the mechanical actuators modify the geometry of the wing, which potentially leads to extra drag and degradation of airfoil performance during off-design conditions.
In frames of the BUTERFLI Project, several groups developed and tested novel approaches for the buffet control on a turbulent supercritical transonic airfoil. Soudakov et al perform investigations of possibility to use tangential jet blowing for buffet control [9]: authors describes a computational effort of buffet phenomenon on supercritical transonic airfoil P-184-15SR and influence of air jet blown continuously from small slot nozzle tangentially to wing upper surface in the region of shock location to reduce shock-induced separation. The study was undertaken to prepare experimental investigations in TsAGI T-112 transonic wind tunnel. Also Sidorenko et al. investigates a spark discharge actuator combined with set of small wedges on wing surface [10] for suppression of buffet. Current work is devoted to application of entirely plasma-based actuators without any mechanical elements.

## 2. Preliminary testing of submicrosecond discharge

### 2.1 Single spark on the surface

The first series of experiments were performed to observe a flow structure of jet-type gas disturbance generated at the decay of the afterspark heated zone near a solid surface. A detailed description of this part of the work can be found in previous publications [11-12]. A universal electrode plate with array of flush-mounted electrodes was designed for a parametric study of the jet characteristics depending on the electric power supply waveform. Typical breakdown voltage was U = 10 kV and peak current up to I = 3 kA. In this experimental series, the results were acquired for single spark mode at the inter-electrode distance of L=7.5 mm. Schlieren visualization was applied for two directions of view for wide range of delay time between the spark and image acquisition: $\Delta t$= 0 μs – 4 ms. Typical schlieren images are presented in Fig.1.
During those experiments a strong anisotropy of the jet was revealed. It was observed that the shapes of gas volume affected by discharge is significantly different for presented plans of view for later time moments t >100μs. The perturbed zone appears in a shape of a half of circle at the enface view and like a jet in a direction normal to surface at the side view. It appears in a form of a half of toroid. This shape of the perturbed region could be explained by

DOI: 10.13009/EUCASS2017-291



initial velocity field of the gas movement in the afterspark area. As it is shown in Fig.1, in plane of electrodes (side view) gas is ejected from sides to the near-electrodes area (to the central area of toroid) and then moves away from this area in the radial direction with the angle of 180°, as it is shown in the plane perpendicular to the spark (enface view). At the early moments after HV breakdown a thermal cavity is rapidly increasing in size, and then the velocity of expansion remains nearly constant. It was found that average speed of the jet interface for the first 20 μs is up to 200 m/s depending on energy input.

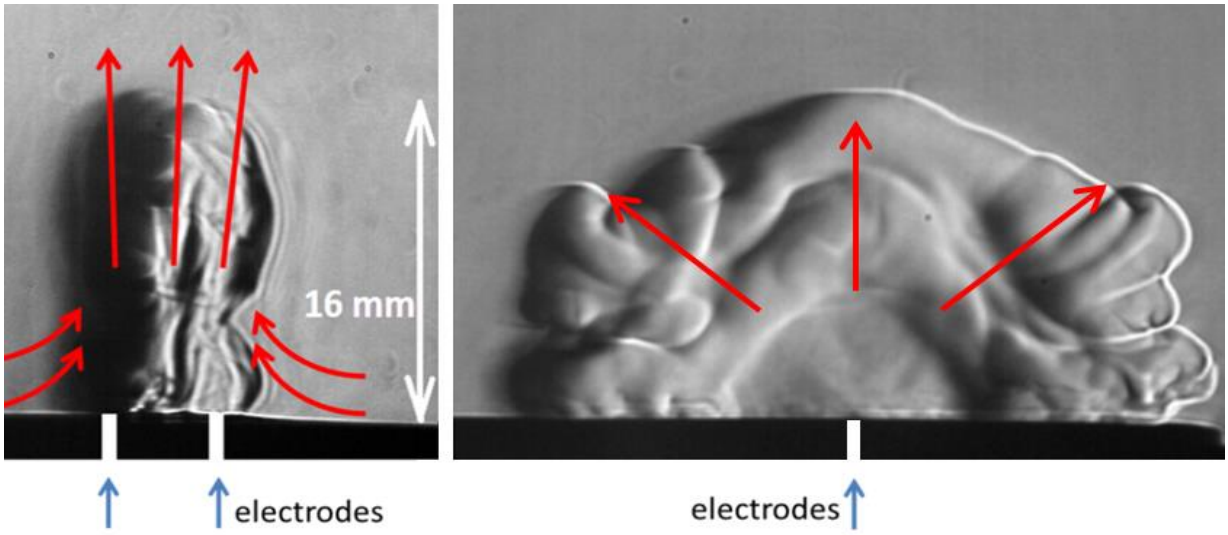


Figure 1. Typical schlieren images for 0.5 ms after breakdown:
side view (left) and enface view (right). Arrows indicate the direction of gas motion.

## 2.2 Testing of multi-spark actuator

In aerodynamic experiment a significant part of wingspan should be affected by simultaneous sparks. For the experiments in wind tunnel at JIHT RAS the model bump has a span of 72 mm; and actuator with 5 spark gaps was successfully checked at one-pulse mode in transonic flow under conditions without buffet, as it was described in [12]. The next model of actuator was prepared for the experiment with transonic buffet on a wing model at TsAGI T-112 wind tunnel. Cross section of the wind tunnel is 0.6x0.6 m that leads to the scheme modification with a higher number of spark gaps operated simultaneously in a pulse-periodic mode. The scheme proposed is shown in Fig. 2(a). Presented scheme was assembled and tested with different number of spark gaps, from 2 to 21. The indicated number of spark gaps (21 pcs) is enough to cover of 300 mm of wingspan by plasma actuator. Operating capacitor is charged to a desired voltage, and then discharged through managed spark gap connected to series connection of spark gaps, each of them is attached to the ground through high resistances $R_{Gr}$. Resistances added to circuit make the breakdown of each gap easier. However, it prevents a major energy release until the complete breakdown through all discharge gaps to the ground. Minimal voltage for stable full breakdown was found as high as U=15 kV for atmospheric pressure. Multiple spark actuator was tested at the pulse-repetitive modes under flow conditions and geometry close to the T-112 wind tunnel tests. At pressure P=0.4 atm for actuator consisted of 21 sparks (0.025 J per spark at one pulse) and for actuator consisted of 18 sparks (0.015 J per spark at one pulse), the maximal obtained frequencies were 1200Hz and 1800Hz respectively, an average power of discharge does not exceed of 650 W. In both cases, the operational frequency was limited by a maximal power of electric power supply. Typical time series of voltage and current for 21 gaps gathered at JIHT chamber without flow are shown in Fig.2(b).

To implement the discharge section to the airfoil model, the dielectric insert was manufactured. The insert consists of Plexiglas base with two patches made by 3D-printing. Assembly contains three inserts of ceramics 44x100 mm; the ground resistors are mounted in the cavity at the downside of the insert. After assembly, the cavity is filled with high-dielectric sealant. Photos of actuators are shown in Fig. 3. Insertion with longitudinal (along the flow) sparks contains 21 pairs of electrodes (1st actuator), and insertion with transverse (across the flow) sparks initially contains 18 pairs of electrodes (2nd actuator) - 3 pairs of electrodes at the end of insertion was disconnected to increase the operation stability.

DOI: 10.13009/EUCASS2017-291



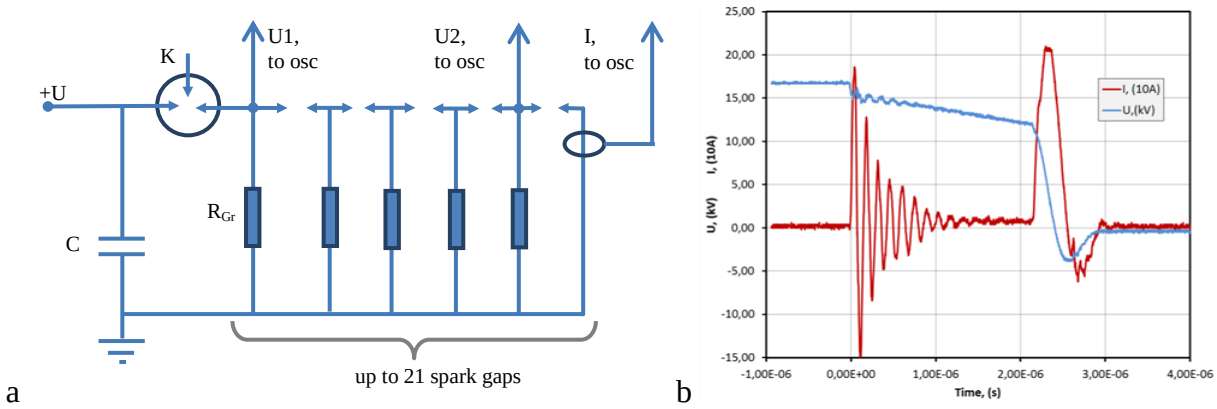


Figure 2. Scheme for multiple simultaneous sparks (a); typical time dependences of voltage and current for 21 gaps without flow in low pressure chamber of JIHT.

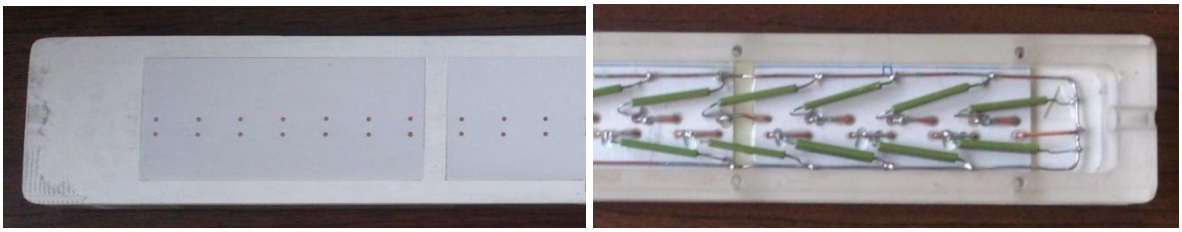

Figure 3. Actuator with 3x(44x100)mm ceramic insertions equipped by 21 pairs of electrodes, longitudinal sparks, top and bottom views.

## 3. Testing of spark actuator in transonic flow

During the preparation of actuator for the aerodynamic tests two basic geometries of the actuator for mounting in the wing model were discussed:

- spark channels are parallel to the streamlines
- spark channels are cross the flow

In both cases the actuator should be located in the middle part of the wing chord upstream and close to the transonic shock.

The aerodynamic tests of spark actuator in transonic flow were performed in TsAGI T-112 wind tunnel with P-184-15SR supercritical airfoil [9] with 200 mm chord. The camera image of wing model equipped by longitudinal spark actuator and installed to wind tunnel is presented in Fig. 4. Tests were carried out at the following range of parameters: AoA=0-60, M=0.73-0.78. The discharge frequencies Fd were tested in a range from 200 to 1180 Hz for 1st actuator at 0.025 J per one spark and in a range from 790 to 1790 Hz for 2nd actuator at 0.015 J per spark. The conclusion about the presence of the buffet was made on the basis of shock oscillations registered by high-speed video camera. In data analysis given below, most attention is given to the tests with high angles of attack and high Mach numbers.

The analysis of pressure distribution doesn't allow making any conclusions on the effect of the discharge on the flow around the wing, because possible decreasing of buffet amplitude could result in the same average pressure distribution. It was obtained that the effect of the discharge on the pressure distributions is negligible: all pressure deviations caused by discharge are within the measurements accuracy.

Schlieren images for different delay time after discharge are presented in Fig.5. As can be seen from Schlieren images, the sparks were located in front of shock or immediately downstream of it, and the discharge thermal cavity expansion takes place behind the shock. This factor can have a dramatic negative effect on the efficiency of the spark-based VG (vortex generator). However, even in this case discharge operation caused no significant effect and even led to a slight decrease in the amplitude of oscillations for several sets of conditions.

DOI: 10.13009/EUCASS2017-291



Figure 4. P-184-15SR wing equipped by longitudinal spark actuator in TsAGI T-112 wind tunnel.

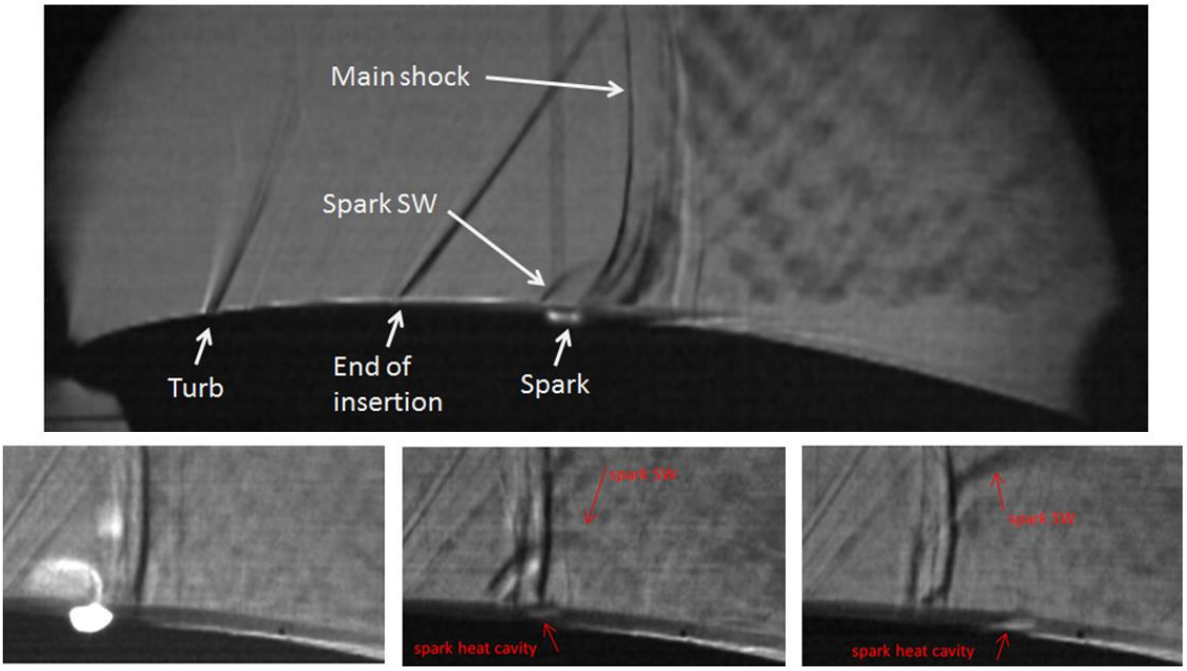


Figure 5. Schlieren images for different delay after discharge.

a

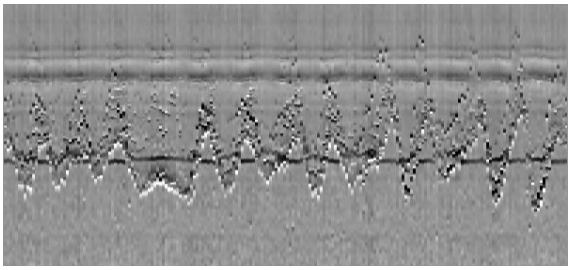

b

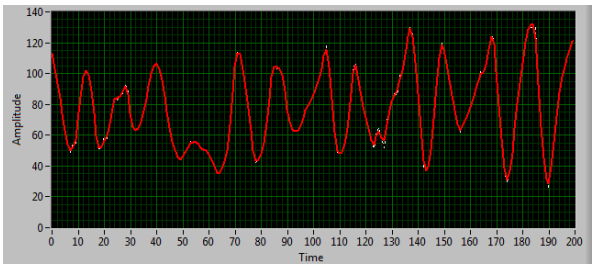


Figure 6. Steps of post-processing:
a – line scan imitation; b – shock motion graph.

DOI: 10.13009/EUCASS2017-291



Following steps of image post-processing were used (see Fig.6). After fast schlieren registration, the imitation of line scan camera image was obtained from each set of snapshots, giving as a result an X-Time diagram of image intensity. Such image contains a curve of the shock oscillation in time. On the next step this image curve is converted to the graph using the method of edge detection. After that for a given graph the amplitude spectrum is constructed and RMS deviation of shock position is calculated.

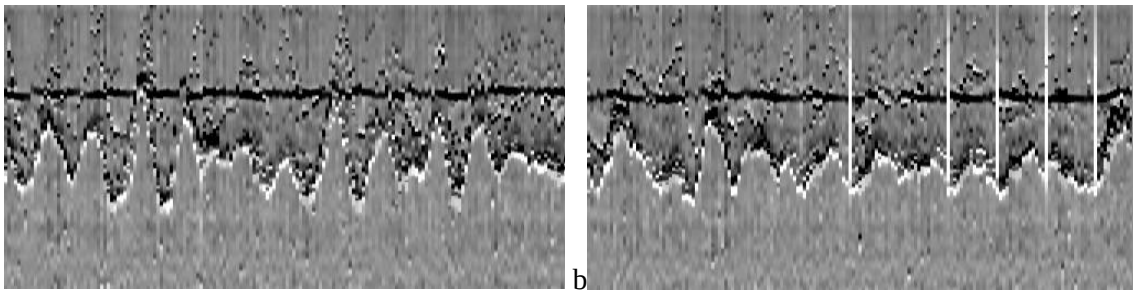

a b

Figure 7. X-Time diagram of image intensity. AoA=5º, M=0.76:
w/o discharge (a) and $F_d$= 400 Hz (b).

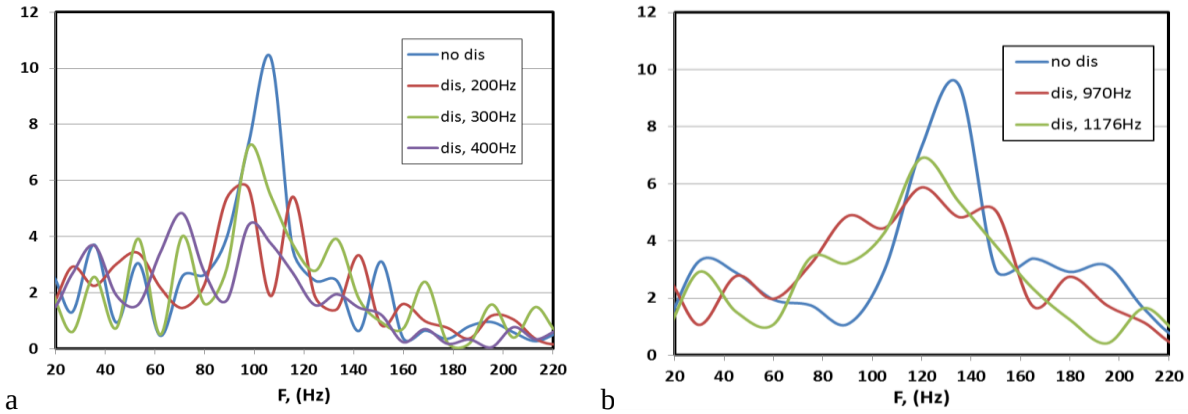


a b

Figure 8. Amplitude spectra: AoA=5º, M=0.76 (a) and AoA=5º, M=0.78 (b).

In conclusion it is necessary to note that there was no effect of discharge on shock position and pressure distribution in case of buffet absence. And moderate effect of decreasing of shock oscillation amplitude (see Fig.7 and Fig.8) was obtained for case of buffet. Further studies are necessary for optimizing the position of the actuator along the wing chord.

## 4. Numerical simulation of spark actuator effect on transonic buffet

Numerical simulation of transonic flow over P-184-15SR supercritical airfoil [9] was carried out by means of FlowVision CFD software on the base of unsteady Reynolds averaged Navier-Stokes (URANS) equations to obtain flow parameters near surface in possible region of spark actuator location and for checking obtained experimental results of actuator influence on buffet. Flow parameters were chosen in accordance with the conditions of TsAGI T-112 wind tunnel and were following: temperature T = 264 K, static pressure Pst = 71090 Pa, Mach number M=0.74, and angle of attack AoA was in range of 4º-6º. Reynolds number based on free-stream parameters and chord length was $Re=2.6\times10^6$. Spalart-Allmaras (SA) or k-ε turbulence model was used for simulations, and computational grid was characterized by dimensionless wall distance Y+ < 1.

As a result of simulation of transonic flow over airfoil at described conditions the buffet effect was achieved. Obtained buffet frequency was 125 Hz for M = 0.74 and AoA=5o that is in a good agreement with experimental one. It was shown that shock oscillation takes place between 43% and 57% of chord length which is 200 mm for airfoil chosen for wind tunnel test (see Fig.9). Three-dimensional simulation of thin layer of wing with one-half of spark was performed to obtain the influence of plasma actuator to the buffet phenomenon. Spark discharge was simulated by volumetric heat source Ø1 mm and length of 3 mm. The energy released by heat source was 0.025 J for complete spark at one pulse, the pulse duration was 1 ms and repetition frequency was equal to 1200 Hz that corresponds to parameters of discharge in the experiment. Two different positions of spark actuator were tested: x/c=0.32 (before shock) and x/c=0.6 (after shock). Wall functions and k-ε turbulence model were used in this simulation, Y+ was lower than 50.

DOI: 10.13009/EUCASS2017-291



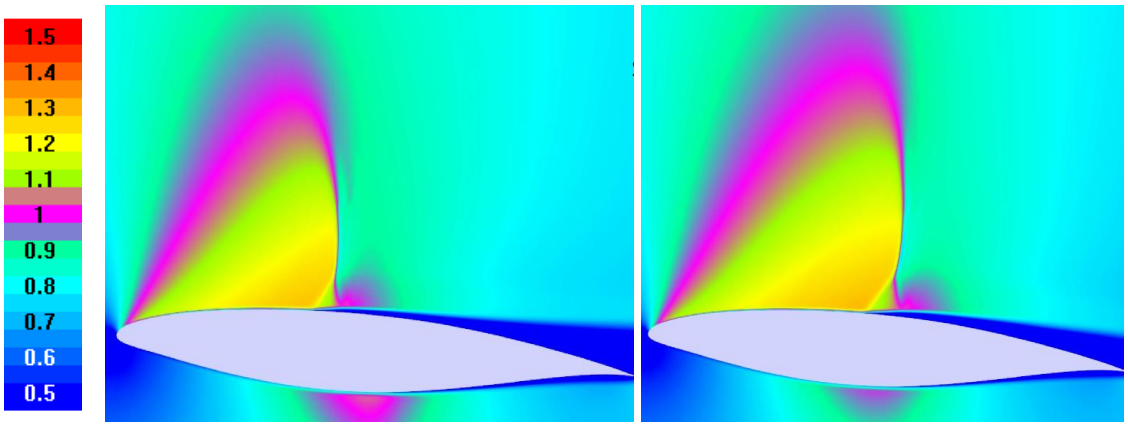


Figure 9. Mach number distributions for minimal and maximal lift force cases during shock oscillation. M=0.74, AoA = 5°. 2D simulation.

For the first case with x/c=0.32, it was found that spanwise velocity Vz achieve up to 70 m/s at 200 μs after discharge pulse and also discharge operation leads to small separation area under the shock foot. This is a confirmation that spark actuator works like vortex generator in transonic flow (see Fig.10). And operation of actuator results in significant amplitude decrease of shock position oscillation (up to 5% of initial amplitude) during 10 periods of buffet with actuator operation. Dependences of shock wave position and lift force vs time are presented in Figure 11. You can see the small bursts on the lift force graph devoted to discharge operation. Moving of discharge to x/c=0.6 leads to insignificant decrease of buffet amplitude in comparison with case without discharge, and disabling of actuator leads to restoration of oscillation amplitude to initial state during 5 periods of buffet.

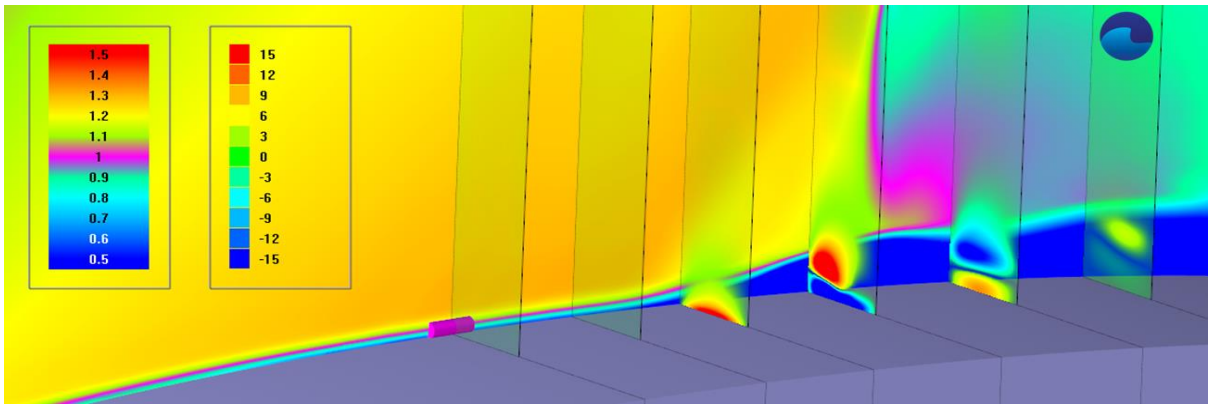


Figure 10. M=0.74, AoA = 5°. 3D simulation, 200 μs after discharge pulse: |Vz| up to 70 m/s. Background colored by Mach number, and YZ-planes colored by Vz.

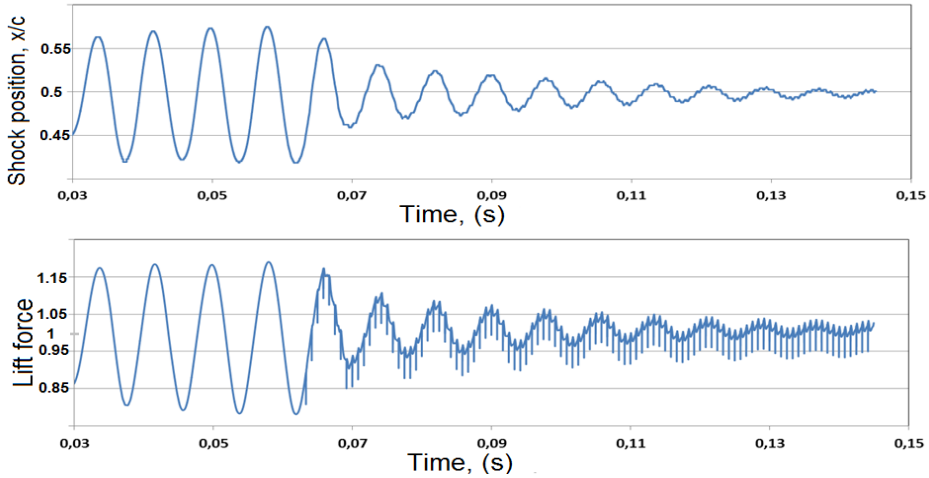


Figure 11. Diminution of shock wave and lift force oscillations after activation of spark actuator. M=0.74, AoA = 5°.

DOI: 10.13009/EUCASS2017-291



## 6. Summary

Experimental and numerical study of implementation of plasma-based flow actuators for control of transonic buffet phenomenon were performed. It was observed that the jet caused by spark actuator has a complex structure with the shape close to the half of toroid. A configuration (practical schematic) of the plasma actuator with multiple simultaneous sparks was developed and successfully tested. The actuator with length of 300 mm contains 21 spark gaps and operates with energy 0.025 J per spark gap, at repetition frequency 1200 Hz, which is one order higher than the buffet frequency. A detectable decrease of the amplitude of oscillations was found after processing of dataset gathered at T-112 wind tunnel tests. The amplitude decrease was predicted by CFD simulation.

## Acknowledgments

Work is performed within the “BUTERFLI” (BUffet and Transition delay control investigated within European-Russian cooperation for improved FLIght performance) project of the 7th Framework Program of European Commission.

## References

[1] Caruana D., Mignosi A., Robitaillie O. C., Correge M. - Separated Flow and Buffeting Control // Flow, Turbulence and Combustion. 2003. V. 71. P. 221–245.

[2] Bur R., Coponet D., Carpels Y. - Separation control by vortex generator devices in a transonic channel flow // Shock Waves. 2009. V. 19. P. 521–530.

[3] Molton P., Bur R., Lepage A., Brunet V., Dandois J. - Control of Buffet Phenomenon on a Transonic Swept Wing // 40th Fluid Dynamics Conference and Exhibit. 2010. 28 June - 1 July, Chicago, Illinois. AIAA 2010-4595.

[4] Dandois J., Brunet V., Molton P., J.-C. Abart, A. Lepage - Buffet Control by Means of Mechanical and Fluidic Vortex Generators // 5th Flow Control Conference. 2010. 28 June - 1 July, Chicago, Illinois. AIAA 2010-4975.

[5] Eastwood J.P., Jarrett J.P. - Toward Designing with Three-Dimensional Bumps for Lift/Drag Improvement and Buffet Alleviation // AIAA J. 2012. V. 50. № 12. P. 2882-2898.

[6] Ogawa H., Babinsky H., Patzold M., Lutz T. - Shock / Boundary-Layer Interaction Control Using Three-dimensional Bumps for Transonic Wings // 45th AIAA Aerospace Sciences Meeting and Exhibit. 2007. 8 - 11 January, Reno, Nevada. AIAA 2007-324.

[7] Caruana D., Mignosi A., Corrège M., Le Pourhiet A., Rodde A.M.,. - Buffet and buffeting control in transonic flow // Aerospace Science and Technology. 2005. V. 9. P. 605-616.

[8] Kogan M.N., Starodubtsev M.A. - Transonic flow past an airfoil with mini-flaps // Fluid Dynamics. 2008. V. 43. № 3. P. 480-484.

[9] Soudakov V.G., Abramova K.A., Brutyan M.A., Lyapunov S.V., Petrov A.V., Potapchik A.V., Ryzhov A.A. - Investigation of buffet control on transonic airfoil by tangential jet blowing // 6th European Conference for Aeronautics and Space Sciences (EUCASS), paper FP-137, 2015

[10] Sidorenko A., Budovsky A., Vishnyakov O., Polivanov P., Maslov A. - Artificial structures in boundary layer and their application for transonic separation control // 6th European Conference for Aeronautics and Space Sciences (EUCASS), paper FP-105, 2015

[11] Firsov A. A., Isaenkov Yu. I., Shurupov M. A., Leonov S. B. - Study of structure and dynamics of gaseous jet after surface spark // 6th European Conference for Aeronautics and Space Sciences (EUCASS), paper FP-190, 2015

[12] Firsov A. A., Isaenkov Yu. I., Shurupov M. A., Leonov S. B. - Development of plasma actuator based on surface sparks for a buffet control // AIAA 2016-1690